



Preparation and Application of Magnetic Fe₃O₄-SBA-15 Mesoporous Silica Adsorbents

SHENGYUN YANG* and GANG YAO

College of Architecture and Environment, Sichuan University, Chengdu 610065, P.R. China

*Corresponding author: Tel/Fax: +86 28 85990967; E-mail: jxskwjh@gmail.com

Received: 6 June 2014;

Accepted: 15 September 2014;

Published online: 27 April 2015;

AJC-17152

Magnetic Fe₃O₄-SBA-15 mesoporous silica molecular sieves were prepared, characterized and used as sorbent for magnetic separation and recycle. Powder X-ray diffraction data indicated that the structure of Fe₃O₄-SBA-15 retained the host SBA-15 structure and Brunauer-Emmett-Teller analysis revealed a increase in surface area and pore size, indicating Fe₃O₄-SBA-15 mixing with the host SBA-15. From scanning electron micrographs, it was found that the structure of the Fe₃O₄-SBA-15 particles changed with the content of Fe₃O₄ and SiO₂. And the Fe₃O₄-SBA-15 exhibited strong magnetic properties. The iron content in Fe₃O₄-SBA-15 was determined by atom adsorption spectroscopy, with the Fe₃O₄ content increased, the capacity of adsorption decreased, but the quality of Fe₃O₄-SBA-15 recycled increased, so we must be controlled the proportion of Fe and Si of Fe₃O₄-SBA-15 mesoporous material, then we could obtain the better material. Fe₃O₄-SBA-15 was successfully used for absorb phenol and recover in water. Our results suggest wide applicability of Fe₃O₄-SBA-15 magnetic mesoporous materials for absorption various compounds in water and recover.

Keywords: Mesoporous material, Fe₃O₄ -SBA-15, Magnetic, Phenol adsorption, Recover.

INTRODUCTION

It is well-known that mesoporous materials have a great interest due to their application in the field of catalysis, fabrication of sensors and adsorption due to their high surface areas and large ordered pores^{1,2}. There are many variety of ordered mesoporous silica materials, such^{3,4} as FSM-16, M41S, MSU⁵, HMS⁶ and SBA⁷ families, which developed using different molecular templates as structure directing agents because of their auto-assembly properties. For example, the mesoporous SBA-15 was synthesized by using amphiphilic triblock copolymers as the structure-directing agents^{8,9}. Mesoporous SBA-15 silica molecular sieves of large pore diameter and area¹⁰ show excellent homogeneity and stability and can be well controlled for adsorption/desorption processes¹¹. There are several routes for modifying interior pore surfaces in mesoporous solids^{12,13} organic functionalization of mesostructured materials has been used to modify the silica surface achieving new applications of these materials in several fields. Recently, mesoporous silica SBA-15 with larger channels and higher thermal and hydrothermal stability than MCM-41 was synthesized by using triblock copolymer as the template^{14,15}. SBA-15 has been explored for synthesis of noble metal Ag, Au, Pt, Ph and Si nanowires¹⁶⁻¹⁹. However, synthesis of binary compound semiconductor nanocrystals and nanowires inside SBA-15 has not been reported.

The SBA-15 material allows to prepare by co-condensation efficient mercury adsorbents. However, SBA-15 is notoriously difficult to separate from solution. Magnetic separation is a useful tool because of its fast recovery, high efficiency and low cost²⁰. Because of their potential applications in this approach, the preparation of Co, Co/Fe, α -Fe₂O₃, α -Fe₂O₃ and Fe₃O₄ magnetic SBA-15 materials have been reported²¹⁻²⁶.

In order to resolve the problems, we selected metal oxide Fe₃O₄ and loaded it into SBA-15 to develop the magnetic materials. We propose a convenient and effective procedure for Fe₃O₄ doping of mesoporous SBA-15 silica because of its excellent magnetic properties. The product was prepared by self-assembly. First, the pores of SBA-15 were doped with iron ions. Then Fe³⁺ was transformed to the oxide form by calcination in the air. Powder X-ray diffraction (XRD), surface area analysis, scanning electron microscopy (SEM), techniques were used to characterize the material. The magnetic properties were demonstrated by using a magnet, the iron content in Fe₃O₄-SBA-15 was determined by atom adsorption spectroscopy (AAS).

EXPERIMENTAL

PluronicP123, poly(ethylene-oxide)20-poly(propyleneoxide) 70-poly(ethyleneoxide)20, was used purchased from A. Tetraethoxysilane (TEOS) was purchased from Shanghai Chemical Reagent (Shanghai, China). Ferric nitrate and the

others chemicals were purchased from Beijing Chemical Reagent (Beijing, China). Ultra pure water (Milli-Q plus, Millipore Inc., Bedford, MA) was used throughout.

Synthesis of the magnetic Fe-SBA-15 mesoporous silica adsorbents: Magnetic Fe-SBA-15 mesostructured silica materials were carried out according to the procedure described by Martinez *et al.*²⁷. In a typical synthesis, pluronic 123 (4 g) was dissolved at room temperature in 125 g of HCl 1.9 M. After heating to 40 °C, 8.6 g TEOS was added to the solution and stirred for periods ranging from 45 min to 8 h. This time is referred to prehydrolysis time of TEOS precursor. The solution was heated up to 40 °C before adding the iron precursor [Fe(NO₃)₃·9H₂O] dissolved in 1.9 M HCl. This mixture was ultrasonication at 40 °C for 2 h. The Si/Fe molar ratio in the synthesis gel was fixed at 30. The material was filtered under low pressure and dried in an oven at 100 °C. Samples were calcined in a muffle furnace at 750 °C for 6 h to obtain a red powder, which was then grind and dried at 800 °C for 6 h. The final product was designated magnetic Fe₃O₄-SBA-15.

Method of characterization: The XRD patterns of powder were obtained with a Bruker D8 Advance X-ray diffractometer using CuK_α radiation at 40 kV and 40 mA. The materials of images were obtained by SEM. The nitrogen adsorption-desorption isotherm measurement was performed on a Micromeritics ASAP 2010 volumetric adsorption analyzer at the temperature of liquid nitrogen. Each spectrum was collected at room temperature under the atmospheric pressure with a resolution of 4 cm⁻¹. The photograph of these devices was obtained by MEIJI three dimensional microscope. The phenol standard curve measure by liquid chromatograph.

RESULTS AND DISCUSSION

Nitrogen adsorption-desorption characterization:

Fig. 1a-c) are shown the N₂ adsorption-desorption isotherms of magnetic Fe₃O₄-SBA-15 of quality percentage Fe₂O₃:SiO₂ (10, 15 and 20 %). The adsorption-desorption isotherm of sample (1, 2) are a typical type IV isotherms with a sharp inflection point at relative pressure P/P₀ 0.4-0.65 due to capillary condensation, as shown in Fig. 1a,b. This inflection is characteristic of mesoporous materials. The isotherms of Fig. 1c is characterized by very steep adsorption into large mesopores, which is associated with the packing voids between nanoparticles in conclusion, the sample^{1,2} are the same size hole of mesoporous material characteristics. The sample 3 channel for the slot hole.

Mesoporous materials of specific surface area, hole volume and hole diameter of physical parameters are shown in Table-1. In Table-1, the samples 1, 2, 3 have specific surface area and the increase of the Fe₂O₃ content can improve the specific surface area and pore volume of the mesoporous materials. Obviously, the small particle size of these samples is responsible for the textural porosity indicated by the hysteresis at high relative pressures. Pore size distribution (PSD) plot shows that three samples have very narrow size distribution, implying highly ordered structure of Fe₃O₄-SBA-15 mesoporous nanoparticles. It is worth noting that the pore size of nanoparticles related to the Fe₂O₃ concentration.

TABLE-1
PHYSICAL PARAMETERS OF MAGNETIC
Fe₃O₄-SBA-15 MESOPOROUS MATERIALS

Sample	Surface area (cm ² g ⁻¹)	Pore volume (cm ³ g ⁻¹)	Pore diameter (nm)
1	348	0.25	3.3
2	472	0.33	3.0
3	460	0.54	4.6

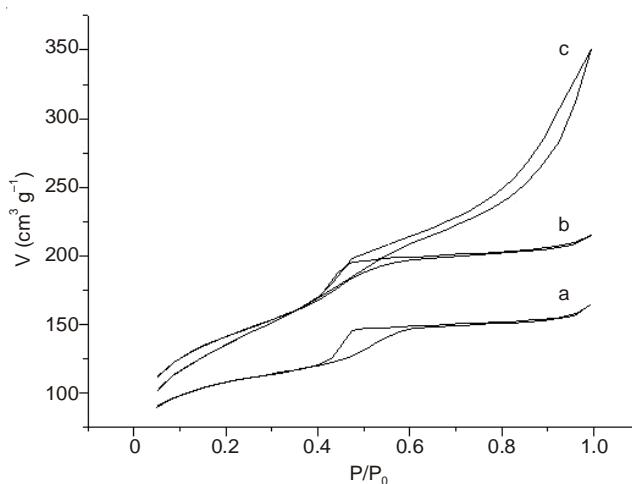


Fig. 1. N₂ adsorption isotherms of magnetic Fe₃O₄-SBA-15

X-ray diffraction: X-ray diffraction patterns of the materials are shown in Fig. 3a-c. For Fe₃O₄-SBA-15, a strong diffraction peaks and two weak diffraction peaks appeared. Comparing to the Fig. 2 of Fe₃O₄ standard card, it can explained SBA-15 original phase six-party mesoporous channel structure not obvious damage, Fe₃O₄/SBA-15 maintained a highly ordered pore structure. Peaks for Fe₃O₄ are evident at 36.5° in the wide-angle XRD pattern for Fe₃O₄-SBA-15. Other peaks can be attributed to Fe₂O₃, Fe or FeO. These results indicate that magnetic Fe₃O₄-SBA-15 still has a high degree of hexagonal symmetry and retains the structure of SBA-15 after calcination at 750 °C and reduction at 800 °C, indicating that SBA-15 has good hydrothermal stability.

Scanning electron microscopy: Scanning electron microscopy images of the different quality percentage Fe₂O₃:SiO₂ (a = 10 %, b = 15 %, c = 20 %) of Fe₃O₄-SBA-15 are shown in

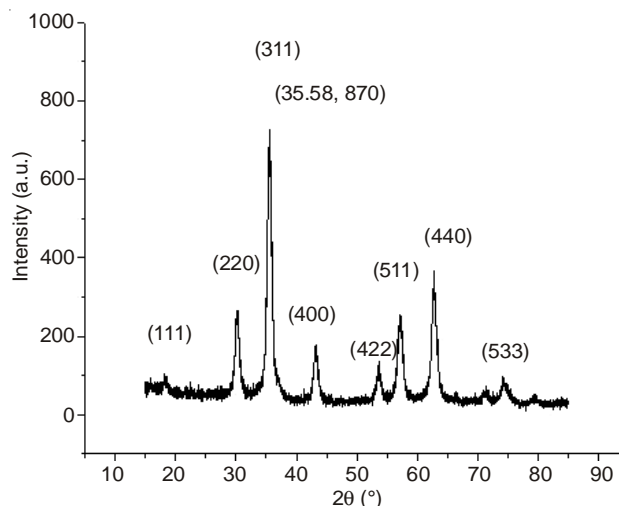


Fig. 2. XRD standard card spectra for Fe₃O₄

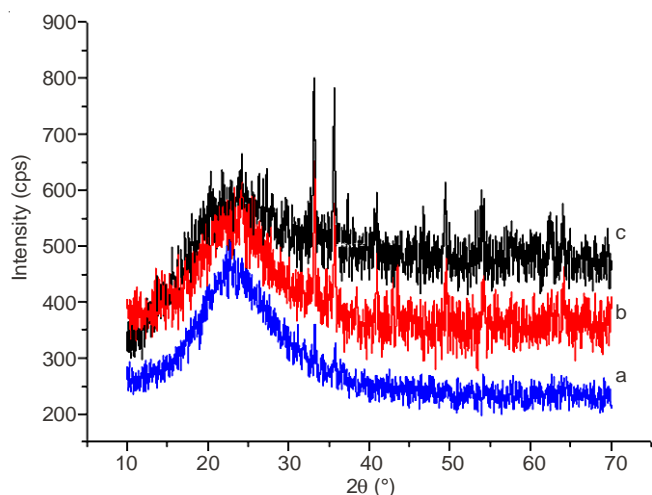


Fig. 3. Powder XRD spectra for mesoporous Fe₃O₄-SBA-15 using the different quality percentage Fe₂O₃: SiO₂ (a = 10 %, b = 15 %, c = 20 %)

Fig. 4. Large fibrous structures of 30-80 μm in length and 10-20 μm in diameter are clearly evident in Fig. 4. Compared to the three images, the shape of these materials is the same on both a microscopic and macroscopic scale, suggesting that the sample of Fe and Si content can change the host SBA-15 structure on ultrasonication. Fig. 5 and Table-2 provide direct evidence that the Fe content and Si content of material. From the calculation the percentage of Si in the prepared materials were 11.57, 12.16 and 10.05 % and Fe in the prepared materials were 0.5, 1.14, 1.88 %, respectively. The above results could also confirm the synthesis of the Fe₃O₄-SBA-15.

Sample	Si content (atomic %)	Fe content (atomic %)
a	11.57	0.50
b	12.16	1.14
c	10.05	1.88

Phenol adsorption experiments: Phenol sets of batch experiments have been carried out to determine the phenol adsorption standard curve. Add 0.25 g phenol to 250 mL volumetric flask and then add H₂O to constant volume, after mixing, add 5, 10, 15, 20 and 25 mL to the front of the prepared of solution in 50 mL volumetric flask respectively, the phenol standard curve by liquid chromatograph of measure. The phenol content was calculated as $A = 0.6644C + 0.8563$ ($R = 0.9917$), where A is the sample absorbance and C is the sample concentration.

Table-3 shows the quality of the adsorption of phenol by Fe₃O₄-SBA-15 (Fe₂O₃:SiO₂; a = 10 %, b = 15 %, c = 20 %). The before the adsorption of phenol solution concentration both of 20 mg/L, but the After the adsorption of phenol solution concentration were 10.62303, 12.42575, 13.34397 mg/L, respectively. The quality of the different content of Fe₃O₄-SBA-15 compare to the phenol were 23.44, 18.94, 16.64 g/mg, respectively. By compared to the result, with Fe₃O₄ content increased, the adsorb content of phenol decreased. It is worth

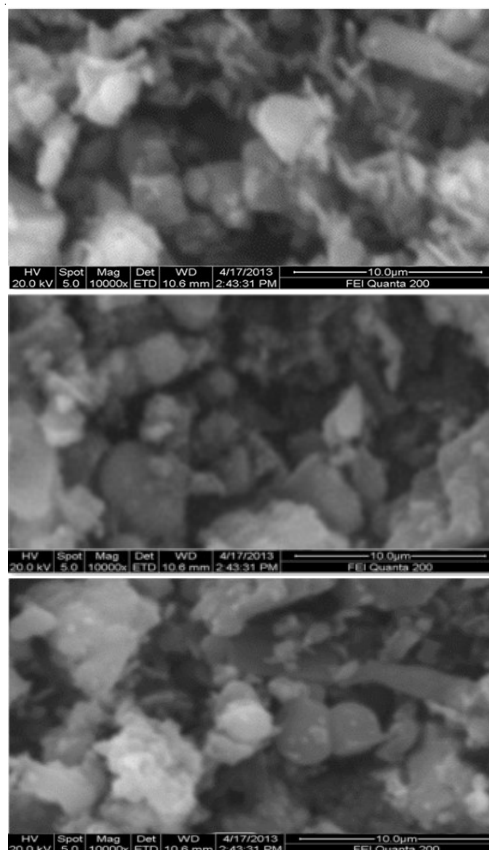


Fig. 4. SEM images of mesoporous Fe₃O₄-SBA-15 using the different quality percentage Fe₂O₃: SiO₂ (a = 10 %, b = 15 %, c = 20 %)

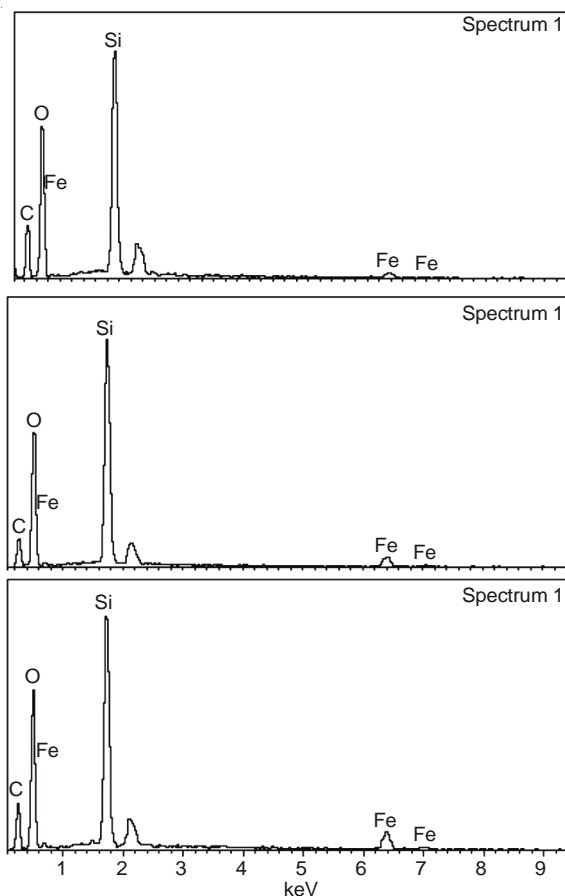


Fig. 5. Fe content of Fe₃O₄-SBA-15 using the different quality percentage

TABLE-3
Fe₃O₄-SBA-15 ADSORB OF PHENOL CONTENT

Sample	Before the adsorption of phenol solution concentration (mg/L)	After the adsorption of phenol solution concentration (mg/L)	Quality of the adsorption of phenol for Fe ₃ O ₄ -SBA-15 (g/mg)
a	20	10.62303	23.44
b	20	12.42575	18.94
c	20	13.34397	16.64

noting that Fe₃O₄-SBA-15 can be used as a sorbent in water. It also demonstrating that Fe₃O₄-SBA-15 can affect the pore permeability of mesoporous materials.

Recycled of magnetic mesoporous Fe₃O₄-SBA-15: Fe₃O₄-SBA-15 exhibited magnetic behaviour with ferromagnet shown in the Fig. 6. Furthermore, it can be seen that the magnetic behavior of Fe₃O₄-SBA-15 was contributed by Fe₃O₄. Because of Fe₃O₄-SBA-15 exhibited strong magnetic behavior, confirming that Fe₃O₄-SBA-15 was magnetic with potential as a magnetic adsorbent for removal from water. Table-4 shows that the rate of recovery of Fe₃O₄-SBA-15 increased, with the Fe₃O₄ content increasing and in accordance with its strong magnetic behavior. There are two possible explanations for the strong magnetic behaviour of Fe₃O₄-SBA-15. First, Fe₃O₄-SBA-15 was prepared with a high content iron. Second, iron may aggregate in SBA-15 channels during calcination and reduction. Large iron metallic particles that formed in Fe₃O₄-SBA-15 can be observed in Fig. 6b.

TABLE-4
QUALITY OF Fe₃O₄-SBA-15 RECYCLED

Sample	Before recover (g)	After recover (g)	Recovery (%)
a	0.1438	0.1129	21.49
b	0.1437	0.0414	71.20
c	0.2161	0.0344	84.08

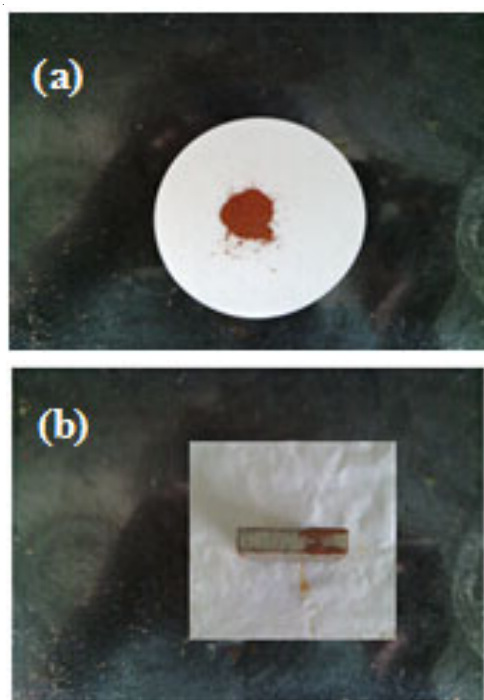


Fig. 6. Photographs of (a) dispersion and (b) magnetic separation of magnetic Fe₃O₄-SBA-15

Conclusion

Magnetic Fe₃O₄-SBA-15 was prepared from mesoporous silica molecular sieves via a simple iron ion doping of SBA-15, transformation to Fe₃O₄-SBA-15. Results confirm that the Fe₃O₄-SBA-15 mesoporous material exhibited magnetic behavior and it can be used to deal with organic wastewater, but it should noting that Fe₃O₄-SBA-15 used as a sorbent. With the Fe₃O₄ content increased, the capacity of adsorption decreased, but the quality of Fe₃O₄-SBA-15 recycled increased, so we must be controlled the proportion of Fe and Si of Fe₃O₄-SBA-15 mesoporous material, then we could obtain the better material.

REFERENCES

1. A. Taguchi and F. Schuth, *Micropor. Mesopor. Mater.*, **77**, 1 (2005).
2. D. Zhao, Q. Huo, J. Feng, B.F. Chmelka and G.D.J. Stucky, *J. Am. Chem. Soc.*, **120**, 6024 (1998).
3. T. Yanagisawa, T. Shimizu, K. Kuroda and C. Kato, *Bull. Chem. Soc. Jpn.*, **63**, 988 (1990).
4. C.T. Kresge, M.E. Leonowicz, W.J. Roth, J.C. Vartuli and J.S. Beck, *Nature*, **359**, 710 (1992).
5. P.T. Tanev and T.J. Pinnavaia, *Science*, **267**, 865 (1995).
6. S.A. Bagshaw, E. Prouzet and T.J. Pinnavaia, *Science*, **269**, 1242 (1995).
7. D. Zhao, J. Feng, Q. Huo, N. Melosh, G.H. Fredrickson, B.F. Chmelka and G.D. Stucky, *Science*, **279**, 548 (1998).
8. D. Zhao, J. Feng, Q. Huo, N. Melosh, G.H. Fredrickson, B.F. Chmelka and G.D. Stucky, *Science*, **279**, 548 (1998).
9. D. Zhao, Q. Huo, J. Feng, B.F. Chmelka and G.D. Stucky, *J. Am. Chem. Soc.*, **120**, 6024 (1998).
10. D. Zhao, J. Feng, Q. Huo, N. Melosh, G.H. Fredrickson, B.F. Chmelka and G.D. Stucky, *Science*, **279**, 548 (1998).
11. J. Zhao, F. Gao, Y. Fu, W. Jin, P. Yang and D. Zhao, *Chem. Commun.*, **7**, 752 (2002).
12. R. Richer and L. Mercier, *Chem. Commun.*, 1175 (1998).
13. F. Babonneau, L. Leite and S. Fontlupt, *J. Mater. Chem.*, **9**, 175 (1999).
14. D. Zhao, J. Feng, Q. Huo, N. Melosh, G.H. Fredrickson, B.F. Chmelka and G.D. Stucky, *Science*, **279**, 548 (1998).
15. D. Zhao, Q. Huo, J. Feng, B.F. Chmelka and G.D.J. Stucky, *J. Am. Chem. Soc.*, **120**, 6024 (1998).
16. Y.J. Han, J.M. Kim and G.D. Stucky, *Chem. Mater.*, **12**, 2068 (2000).
17. M.H. Huang, A. Choudrey and P. Yang, *Chem. Commun.*, 1063 (2000).
18. N.R.B. Coleman, N. O'Sullivan, K.M. Ryan, T.A. Crowley, M.A. Morris, T.R. Spalding, D.C. Steytler and J.D.J. Holmes, *J. Am. Chem. Soc.*, **123**, 7010 (2001).
19. A. Fukuoka, Y. Sakamoto, S. Guan, S. Inagaki, N. Sugimoto, Y. Fukushima, K. Hirahara, S. Iijima and M.J. Ichikawa, *J. Am. Chem. Soc.*, **123**, 3373 (2001).
20. Y. Zhang, R. Liu, Y. Hu and G. Li, *Anal. Chem.*, **81**, 967 (2009).
21. A.N.H. Lu, W. Schmidt, N. Matoussevitch, H. Bönemann, B. Spliethoff, B. Tesche, E. Bill, W. Kiefer and F. Schüth, *Angew. Chem. Int. Ed.*, **43**, 4303 (2004).
22. A.N.H. Lu, W.C. Li, A. Kiefer, W. Schmidt, E. Bill, G. Fink and F. Schüth, *J. Am. Chem. Soc.*, **126**, 8616 (2004).
23. Y. Du, S. Liu, Y. Ji, Y. Zhang, N.I. Xiao and F.-S. Xiao, *J. Magn. Magn. Mater.*, **320**, 1932 (2008).
24. H.X. Jin, L. Li, N.J. Chu, Y.P. Liu, L.Y. Wang, Q. Lu, J. Qian, L.N. Sun, Q. Tang, H.L. Ge and X.Q. Wang, *Mater. Chem. Phys.*, **112**, 112 (2008).
25. J.S. Jung, K.H. Choi, Y.K. Jung, S.H. Lee, V.O. Golub, L. Malkinski and C.J. O'Connor, *J. Magn. Magn. Mater.*, **272-276**, E1157 (2004).
26. H.H.P. Yiu, M.A. Keane, Z.A.D. Lethbridge, M.R. Lees, A.J. El Haj and J. Dobson, *Nanotechnology*, **19**, 255606 (2008).
27. F. Martinez, Y.-J. Han, G. Stucky, J.L. Sotelo, G. Ovejero and J.A. Melero, *Stud. Surf. Sci. Catal.*, **142**, 1109 (2002).